INTERNATIONAL JOURNAL FOR NUMERICAL METHODS IN FLUIDS, VOL. 4, 931–947 (1984)

# TWO-STEP EXPLICIT FINITE ELEMENT METHOD FOR TWO-LAYER FLOW ANALYSIS

KOICHI KASAHARA
*Mitsui Engineering & Shipbuilding Co., Ltd., 6–4, Tsukiji 5-Chome, Chuo-ku, Tokyo, Japan*

HEIHACHIRO HARA
*Mitsui Engineering & Shipbuilding Co., Ltd., 16–1, Tamahara 3-Chome, Tamano-shi, Okayama, Japan*

AND

MUTSUTO KAWAHARA
*Department of Civil Engineering, Chuo University, Kasuga 1-Chome 13, Bunkyo-ku, Tokyo, Japan*

## SUMMARY

A finite element method for the analysis of two-layer density flows is presented in this paper. The standard Galerkin method based on linear interpolation functions is used to yield discrete spatial variables. For numerical integration in time, an explicit two-step selective lumping method is used. Here it is applied to a flow analysis of Ishikari Bay, at the mouth of Ishikari River. This case demonstrates a procedure that yields a numerically stable solution.

KEY WORDS Two-layer Flow Two-step Scheme Selective Lumping Method Ishikari Bay

## INTRODUCTION

The tide marks for many of the estuaries along the Japan Sea coast are quite narrow. In such estuaries, there is incomplete mixing of salt and fresh water. They are classified as fully stratified estuaries. These waters always require two-layer flow analyses.

Recently a number of finite element methods have been applied to analyse shallow water equations. The analysis may be divided into three groups: steady flow, [1–4] quasi-steady flow,[5–11] and unsteady flow analyses.[12–21] There are several papers which discuss multiple-level flow analysis.[22,23] However, in practice, there are many problems which can be analysed by a two-layer flow model. This paper describes unsteady two-layer flows using the finite element method. An explicit two-step selective lumping method is used as the time marching scheme. This scheme, a modified two-step Lax–Wendroff method, has been extensively investigated by Kawahara *et al.*[24] The advantage of using the method is that core store and computation time can be saved. Linear functions of the triangular finite element are adopted as interpolation functions for both velocities and water elevations.

The method described here is applied to a flow analysis of Ishikari Bay including the estuary of the Ishikari River located in western Hokkaido in the northern part of Japan. Generally, it is impossible to obtain a steady flow solution whenever the boundary conditions are not sufficiently given. In actual cases, however, it is seldom that boundary conditions are adequately given because of a lack of observed data. Here, the procedure for adjusting the flow demonstrates a way to overcome such shortcomings.

0271–2091/84/100931–17$01.70

*Received 2 February 1983*
*Revised 21 September 1983*

## BASIC EQUATIONS

The basic equations governing two-layer density flow can be derived from the three-dimensional Navier–Stokes equations, in a manner similar to that used in the shallow water theory, assuming the hydrostatic pressure distribution and integrating these equations over the depth of each layer. Throughout this paper, indicial notation and the usual summation convention are used, and the notation, $(\ )_{,i}$ means partial differentiation with respect to co-ordinate $x_i$. The equations of motion and continuity may be written for the upper layer,

$$\dot{U}_i^{\mathrm{u}} + U_j^{\mathrm{u}} U_{i,j}^{\mathrm{u}} + g\eta_{,i} + F\varepsilon^{ji} U_j^{\mathrm{u}} - A^{\mathrm{u}}(U_{i,j}^{\mathrm{u}} + U_{j,i}^{\mathrm{u}})_{,j} - \frac{1}{\rho^{\mathrm{u}} H^{\mathrm{u}}}(\tau_i^{\mathrm{Su}} - \tau_i^{\mathrm{Bu}}) = 0 \tag{1}$$

$$\dot{\eta} + (H^{\mathrm{u}} U_i^{\mathrm{u}})_{,i} + (H^{\mathrm{l}} U_i^{\mathrm{l}})_{,i} = 0 \tag{2}$$

and for the lower layer,

$$\dot{U}_i^{\mathrm{l}} + U_j^{\mathrm{l}} U_{i,j}^{\mathrm{l}} + g\left(\frac{\rho^{\mathrm{u}}}{\rho^{\mathrm{l}}}\eta_{,i} - \left(1 - \frac{\rho^{\mathrm{u}}}{\rho^{\mathrm{l}}}\right) d_{,i}\right) + F\varepsilon^{ji} U_j^{\mathrm{l}} - A^{\mathrm{l}}(U_{i,j}^{\mathrm{l}} + U_{j,i}^{\mathrm{l}})_{,j} - \frac{1}{\rho^{\mathrm{l}} H^{\mathrm{l}}}(\tau_i^{\mathrm{Sl}} - \tau_i^{\mathrm{Bl}}) = 0 \tag{3}$$

$$-\dot{d} + (H^{\mathrm{l}} U_i^{\mathrm{l}})_{,i} = 0 \tag{4}$$

where, referring to Figure 1, $U_i$ indicates velocity components, $\eta$ represents surface water elevations, $d$ represents interface water elevations, $g$, $\rho$, $F$ and $A$ denote gravity acceleration, water density, Coriolis parameter and coefficient of eddy kinematic viscosity, respectively, and $\varepsilon^{ij}$ indicates the two-dimensional permutation symbol; $\varepsilon^{12} = -\varepsilon^{21} = 1$, $\varepsilon^{11} = \varepsilon^{22} = 0$.

Superscripts u and l denote upper and lower layers, respectively. Unless otherwise stated, Latin indices represent the numbers, 1 and 2.

The letter $H$ designates layer thicknesses, for example

$$H^{\mathrm{u}} = \eta + d, \quad H^{\mathrm{l}} = h - d \tag{5}$$

$\tau_i^{\mathrm{S}}$ and $\tau_i^{\mathrm{B}}$ denote shearing stress components at the surface and at the bottom of each layer:

$$\tau_i^{\mathrm{Su}} = k_{\mathrm{s}}^2 \rho_{\mathrm{a}} W_i (W_j W_j)^{1/2} \tag{6}$$

$$\begin{aligned} \tau_i^{\mathrm{Bu}} &= k_{\mathrm{m}}^2 \rho^{\mathrm{u}} (U_i^{\mathrm{u}} - U_i^{\mathrm{l}})((U_j^{\mathrm{u}} - U_j^{\mathrm{l}})(U_j^{\mathrm{u}} - U_j^{\mathrm{l}}))^{1/2} \\ \tau_i^{\mathrm{Sl}} &= k_{\mathrm{m}}^2 \rho^{\mathrm{l}} (U_i^{\mathrm{u}} - U_i^{\mathrm{l}})((U_j^{\mathrm{u}} - U_j^{\mathrm{l}})(U_j^{\mathrm{u}} - U_j^{\mathrm{l}}))^{1/2} \end{aligned} \tag{7}$$

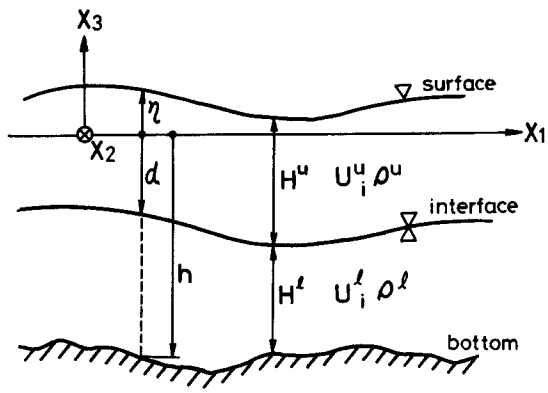


Figure 1. Geometrical definition of two-layer flow

$$\tau_i^{Bl} = k_b^2 \rho^l U_i^l (U_j^l U_j^l)^{1/2} \tag{8}$$

where $k_s^2$, $k_m^2$ and $k_b^2$ represent friction coefficients at the surface, at the interface and at the bottom, respectively. $\rho_a$ is air density and $W_i$ denotes the wind velocity component. The boundary conditions are, on the upper layer boundary, $S^u$,

$$U_i^u = \hat{U}_i^u \qquad \text{on } S_1^u \tag{9}$$

$$q_i^u = A^u(U_{i,j}^u + U_{j,i}^u)n_j = \hat{q}_i \qquad \text{on } S_2^u \tag{10}$$

$$\eta = \hat{\eta} \qquad \text{on } S_3^u \tag{11}$$

where $n_j$ is a unit normal to the boundary surface and a superposed circumflex ($\hat{}$) denotes the prescribed value on the boundary. On the lower layer boundary, $S^l$, similar conditions are imposed.

## FINITE ELEMENT FORMULATION

The domain to be analysed is idealized to consist of subdomains called finite elements. The values of $U_i$, $d$ and $\eta$ at the nodes are taken as field variables. Applying the conventional finite element procedure, equations (1)–(4) are transformed to a set of non-linear simultaneous equations as follows:

$$M_{mn}\dot{U}_{ni}^u + K_{mnkj}U_{nj}^u U_{ki}^u + gB_{mni}\eta_n + M_{mn}F\varepsilon^{ji}U_{nj}^u + C_{mjni}U_{nj}^u - N_m T_i^u = 0 \tag{12}$$

$$M_{mn}\dot{\eta}_n + P_{mnki}((\eta_n + d_n)U_{ki}^u + (h_n - d_n)u_{ki}^l) = 0 \tag{13}$$

$$M_{mn}\dot{U}_{ni}^l + K_{mnkj}U_{nj}^l U_{ki}^l + gB_{mni}\left(\frac{\rho^u}{\rho^l}\eta_n - \left(1 - \frac{\rho^u}{\rho^l}\right)d_n\right) + M_{mn}F\varepsilon^{ji}U_{nj}^l + C_{mjni}U_{nj}^l - N_m T_i^l = 0 \tag{14}$$

$$-M_{mn}\dot{d}_n + P_{mnki}(h_n - d_n)U_{ki}^l = 0 \tag{15}$$

where

$$M_{mn} = \int_v \Phi_m \Phi_n \mathrm{d}V, \qquad K_{mnki} = \int_v \Phi_m \Phi_n \Phi_{k,i}\mathrm{d}V \tag{16}$$

$$N_m = \int_v \Phi_m \mathrm{d}V, \qquad B_{mni} = \int_v \Phi_m \Phi_{n,i}\mathrm{d}V$$

$$C_{mjni} = \int_v (\Phi_{m,j}\Phi_{n,i} + \Phi_{m,k}\Phi_{n,k}\delta_{ij})\mathrm{d}V.A$$

$$P_{mnki} = \int_v \Phi_m(\Phi_{n,i}\Phi_k + \Phi_n\Phi_{k,i})\mathrm{d}V$$

$$T_i^u = \frac{1}{\rho^u H^u}(\tau_i^{Su} - \tau_i^{Bu}), \qquad T_i^l = \frac{1}{\rho^l H^l}(\tau_i^{Sl} - \tau_i^{Bl}) \tag{17}$$

where $\Phi_m$ denotes an interpolation function and $\delta_{ij}$ represents the Kronecker delta. In this paper, linear interpolation functions based on the three-node triangular element are employed.

For numerical integration in time, an explicit two-step selective lumping method[22] is adopted. Applying this procedure, which consists of two steps, to equations (12)–(15), the following relations are obtained:

For the first step,

$$\bar{M}_{mn}U^{u\,n+1/2}_{ni} = \bar{M}_{mn}U^{u\,n}_{ni} - \frac{\Delta t}{2}(K_{mnkj}U^{u\,n}_{nj}U^{u\,n}_{ki} + gB_{mni}\eta^n_n + M_{mn}F\varepsilon^{ji}U^{u\,n}_{nj} + C_{mjni}U^{u\,n}_{nj} - N_m T^{un}_i) \tag{18}$$

$$\bar{M}_{mn}\eta^{n+1/2}_n = \tilde{M}_{mn}\eta^n_n - \frac{\Delta t}{2}(P_{mnki}((\eta^n_n + d^n_n)U^{l\,n}_{ki} + (h^n_n - d^n_n)U^{l\,n}_{ki})) \tag{19}$$

$$\bar{M}_{mn}U^{l\,n+1/2}_{ni} = \bar{M}_{mn}U^{l\,n}_{ni} - \frac{\Delta t}{2}(K_{mnkj}U^{l\,n}_{nj}U^{l\,n}_{ki} + gB_{mni}\left(\frac{\rho^u}{\rho^l}\eta^n_n - \left(1 - \frac{\rho^u}{\rho^l}\right)d^n_n\right) + M_{mn}F\varepsilon^{ji}U^{l\,n}_{nj} + C_{mjni}U^{l\,n}_{nj} - N_m T^{ln}_i) \tag{20}$$

$$\bar{M}_{mn}d^{n+1/2}_n = \tilde{M}_{mn}d^n_n + \frac{\Delta t}{2}(P_{mnki}(h^n_n - d^n_n)U^{l\,n}_{ki}) \tag{21}$$

and for the second step,

$$\bar{M}_{mn}U^{u\,n+1}_{ni} = \bar{M}_{mn}U^{u\,n}_{ni} - \Delta t(K_{mnkj}U^{u\,n+1/2}_{nj}U^{u\,n+1/2}_{ki} + gB_{mni}\eta^{n+1/2}_n + M_{mn}F\varepsilon^{ji}U^{u\,n+1/2}_{nj} + C_{mjni}U^{u\,n}_{nj} - N_m T^{u\,n+1/2}_i) \tag{22}$$

$$\bar{M}_{mn}\eta^{n+1}_n = \tilde{M}_{mn}\eta^n_n - \Delta t(P_{mnki}((\eta^{n+1/2}_n + d^{n+1/2}_n)U^{u\,n+1/2}_{ki} + (h^{n+1/2}_n - d^{n+1/2}_n)U^{l\,n+1/2}_{ki})) \tag{23}$$

$$\bar{M}_{mn}U^{l\,n+1}_{ni} = \bar{M}_{mn}U^{l\,n}_{ni} - \Delta t(K_{mnki}U^{l\,n+1/2}_{nj}U^{l\,n+1/2}_{ki} + gB_{mni}\left(\frac{\rho^u}{\rho^l}\eta^{n+1/2}_n - \left(1 - \frac{\rho^u}{\rho^l}\right)d^{n+1/2}_n\right) + M_{mn}F\varepsilon^{ji}U^{l\,n+1/2}_{nj} + C_{mjni}U^{l\,n}_{nj} - N_m T^{l\,n+1/2}_i) \tag{24}$$

$$\bar{M}_{mn}d^{n+1}_n = \tilde{M}_{mn}d^n_n + \Delta t(P_{mnki}(h^{n+1/2}_n - d^{n+1/2}_n)U^{l\,n+1/2}_{ki}) \tag{25}$$

where the superscript $n$ indicates the value at the $n$th time step and $\bar{M}_{mn}$ denotes the lumped coefficient. $\tilde{M}_{mn}$ is defined as follows:

$$\tilde{M}_{mn} = e\bar{M}_{mn} + (1 - e)M_{mn} \tag{26}$$

where $e$ represents the selective lumping parameter.

## APPLICATION TO ISHIKARI BAY

Ishikari Bay is located in western Hokkaido on the Sea of Japan (Figure 2). The Ishikari River, one of the largest rivers of Japan, flows into this bay. The narrow tidal range in the bay, no more than 30cm, results in a salt-wedge in the estuary classified as a 'weak mixing' type. Observations show that this estuary has both salt water and fresh water strata. In the dry season the tip of the salt-wedge may intrude upstream more than 10 km from the river mouth.[25-27] Therefore, in order to analyse the flow phenomena in this area, especially in the neighbourhood of the river mouth, it is necessary to apply to two-layer flow analysis.

Steady flow is calculated taking into account flow patterns in this coastal sea. The finite element idealization is illustrated in Figure 3. The scale of the selected domain is about 17 km from north to

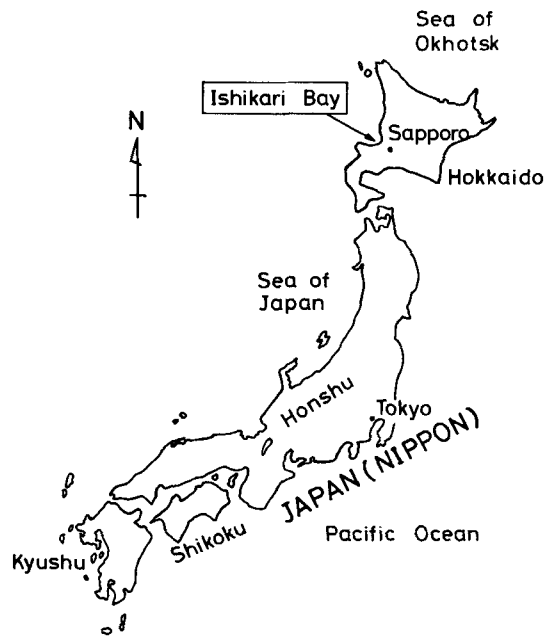


Figure 2. Location

south, and about 10 km from east to west. The total number of finite elements is 1024 and the total number of nodal points is 576 for each layer.

After several trials, boundary conditions were determined as shown in Table I and Figure 4. Physical constants and computational data are presented in Table II. Under such conditions, computation was carried out up to 1800 loops.

Figure 5 shows the time history curves of $U$, $\eta$ and $d$ at the selected points. However, it is difficult to say that this result is in a steady state because the water elevations $\eta$ and $d$ are fluctuating. So, to get a steady state solution, better means of approach was considered as discussed later. Finally, by means of this approach, we succeeded in getting a steady state solution as shown in Figure 8. Next, a procedure adopted in this study is explained in detail.

Reflecting on the above result, this phenomenon is attributed to inadequate boundary conditions. Because of a lack of observed data, it is impossible to specify the interface boundary conditions on the offshore boundary. Accordingly, it is not possible to maintain a balance between inflow and outflow in the area analysed in the sense of steady flow. Thus, the water elevations $\eta$ and $d$ are supposed to decrease and increase in order to maintain the steady state, because the inflow discharge must be increasing. From the above discussions, it is necessary to introduce a procedure for adjusting the inflow.

*Adjustment of inflow*

In order to obtain a steady flow solution by means of adjusting the inflow, the flow quantity to be adjusted must be estimated. The following estimation method is proposed:

Let $\dot{Q}_{st}$ be inflow per unit time to maintain a steady flow state, $Q$ be inflow per unit time at an arbitrary time and $\Delta\dot{Q}$ be the adjusted inflow, then the following relation is obtained:

$$\dot{Q}_{st} = \dot{Q} + \Delta\dot{Q} \tag{27}$$

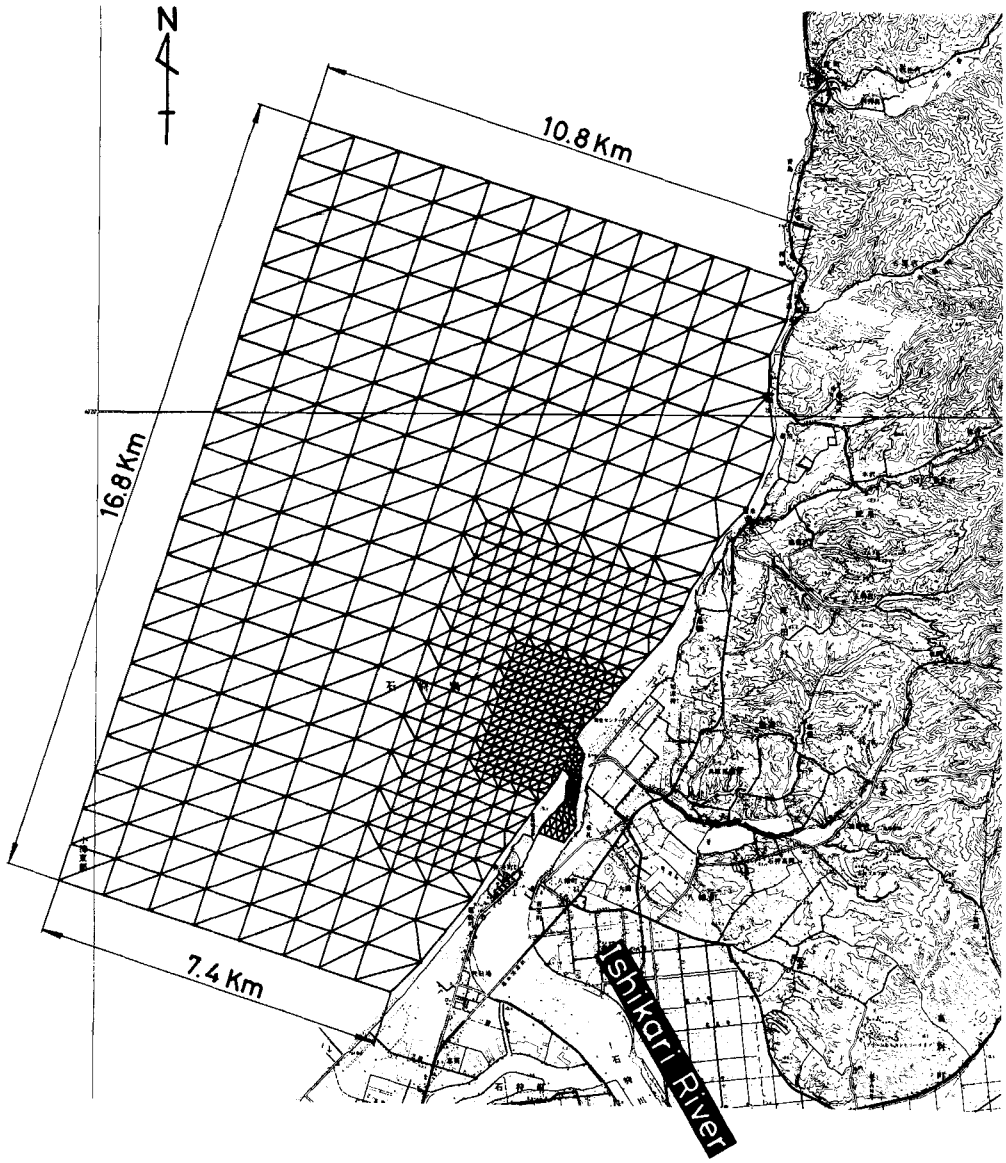


Figure 3. Finite element idealization

Table I. Boundary conditions

| Location Figure 4 | Boundary conditions: Water elevations $\eta$, $d$ (m) | | Velocities $U$ (m/s) | | Remarks |
|---|---|---|---|---|---|
| ABCDEF | $\eta + d$ | 0·12 (at A)<br>0·14 (at B)<br>0·10 (at C)<br>0·14 (at D)<br>0·04 (at E)<br>0·04 (at F) | $U^l$ | 0·123 (at A)<br>0·25 (at C)<br>0·25 (at E)<br>0·114 (at F) | Interpolated linearly between locations |
| GH | $\eta + d$ | 3·5 | $U^u$ | 0·15 | River discharge $= 300\,m^3/s$ |
| FG and HA | — | — | $U^l$ | 0·0 | (see Reference 25) |
| | | | $U_n^u$ | 0·0 | $U_n$ Normal velocity component to shoreline |
| | | | $U_n^l$ | 0·0 | |

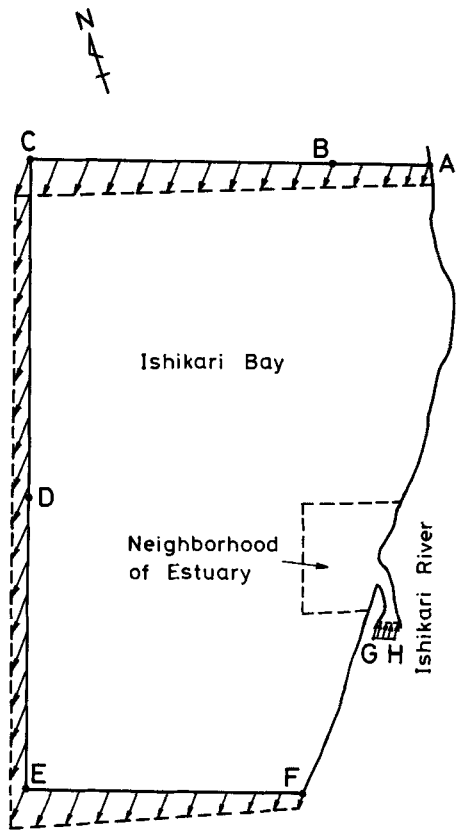


Figure 4. Boundary conditions for analysis of Ishikari Bay (cf. Table I)

Table II. Physical constants and computational data

| | |
|---|---|
| Density of upper layer | $\rho^u = 1{\cdot}0 \times 10^3\,\mathrm{kg/m^3}$ |
| Density of lower layer | $\rho^l = 1{\cdot}024 \times 10^3\,\mathrm{kg/m^3}$ |
| Coriolis parameter | $F = 9{\cdot}974 \times 10^{-5}\,1/\mathrm{s}$ |
| Friction coefficient at the interface | $k_m^2 = 0{\cdot}001\,\mathrm{m/s}$ |
| Friction coefficient at the bottom | $k_b^2 = 0{\cdot}0026\,\mathrm{m/s}$ |
| Coefficient of eddy kinematic viscosity | $A = 10{\cdot}0\,\mathrm{m^2/s}$ |
| Selective lumping factor | $e = 0{\cdot}0$ |
| Time increment | $\Delta t = 6{\cdot}0\,\mathrm{s}$ |

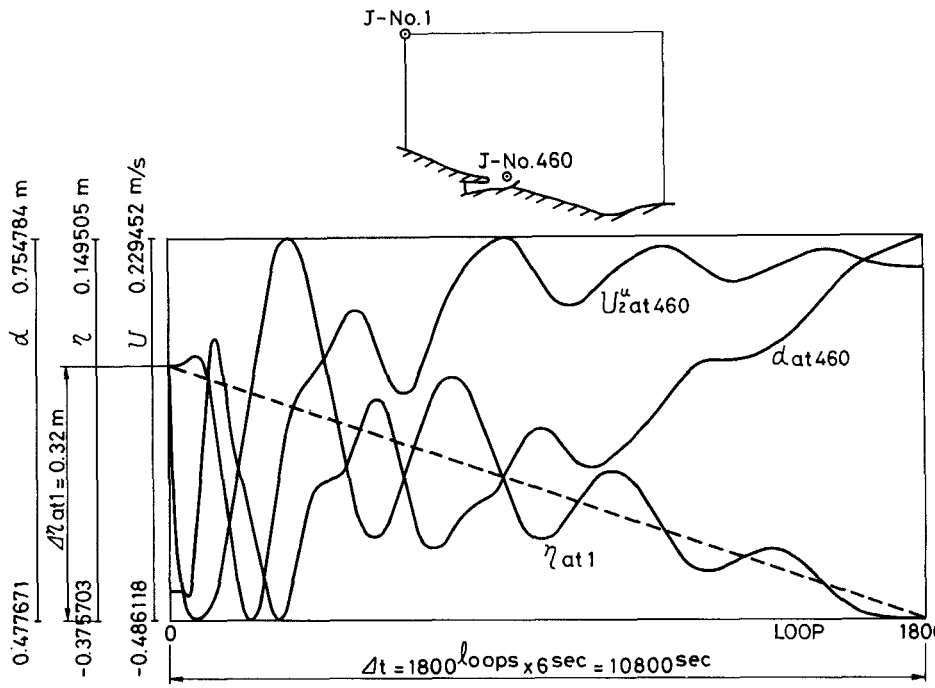


Figure 5. Time history curves of $U_2^u$ (at J-No. 460), $\eta$ (at J-No. 1) and $d$ (at J-No. 460) (original)

$$\Delta\dot{Q} = \dot{\eta}A \tag{28}$$

where $\dot{\eta}$ is the rate of surface water elevation change per unit time, and $A$ is the total area of the domain to be analysed (Figure 6). From the time history curve of $\eta$, by reading $\Delta\eta$ and $\Delta t$, $\dot{\eta}$ may be obtained as follows:

$$\dot{\eta} = \frac{\Delta\eta}{\Delta t} \tag{29}$$

Because the fluid in the lower layer flows into the domain only across the boundary AC, $\dot{Q}$ can be

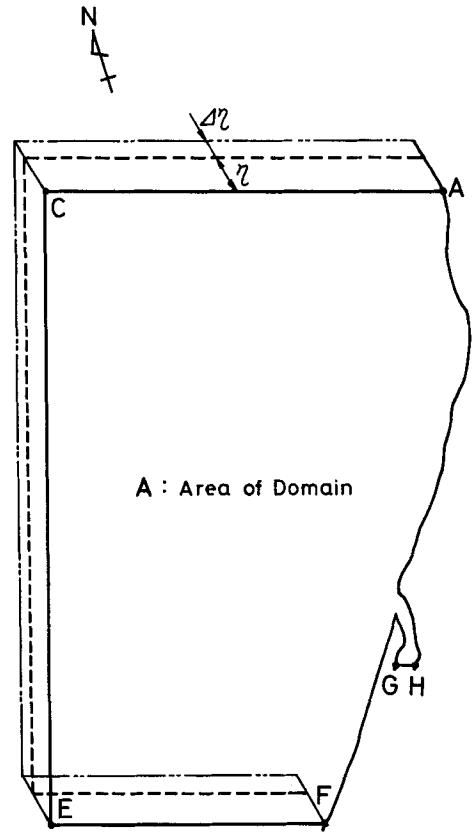


Figure 6. Water elevation change

calculated from the following equation:

$$\dot{Q} = \int_{A}^{C} H^{1} U^{1} \mathrm{d}l \tag{30}$$

Using this method, the inflow discharge, i.e. the velocities of the lower layer on AC, can be adjusted.

*First modification*

From the time history curve of the preceding trial (Figure 5), $\Delta\eta$ and $\Delta t$ can be read, then $\dot{\eta}$ is obtained, i.e. $\Delta\eta_{\mathrm{at}\,1} = 0{\cdot}32$ m, $\Delta t = 1800$ loops $\times$ 6 s $= 10800$ s.

Therefore, the rate of surface water elevation change per unit time at nodal point No. 1 is $\dot{\eta}_{\mathrm{at}\,1} = \Delta\eta_{\mathrm{at}\,1}/\Delta t = 2{\cdot}963 \times 10^{-5}$ m/s. As an average for the whole region, the following value is assumed: $\dot{\eta} = 3 \times 10^{-5}$ m/s. Hence, $\dot{Q}_{\mathrm{st}}/\dot{Q} = 1{\cdot}105$. So, the prescribed values of velocities of the lower layer on AC should be increased by 10 per cent.

As the initial condition, the result of loop No. 1100 of the preceding trial was used. As a result, Figure 7 shows that the water elevations $\eta$ and $d$ are considerably improved compared with the previous computation. However, if these still fluctuate slightly, one more adjustment might be necessary.

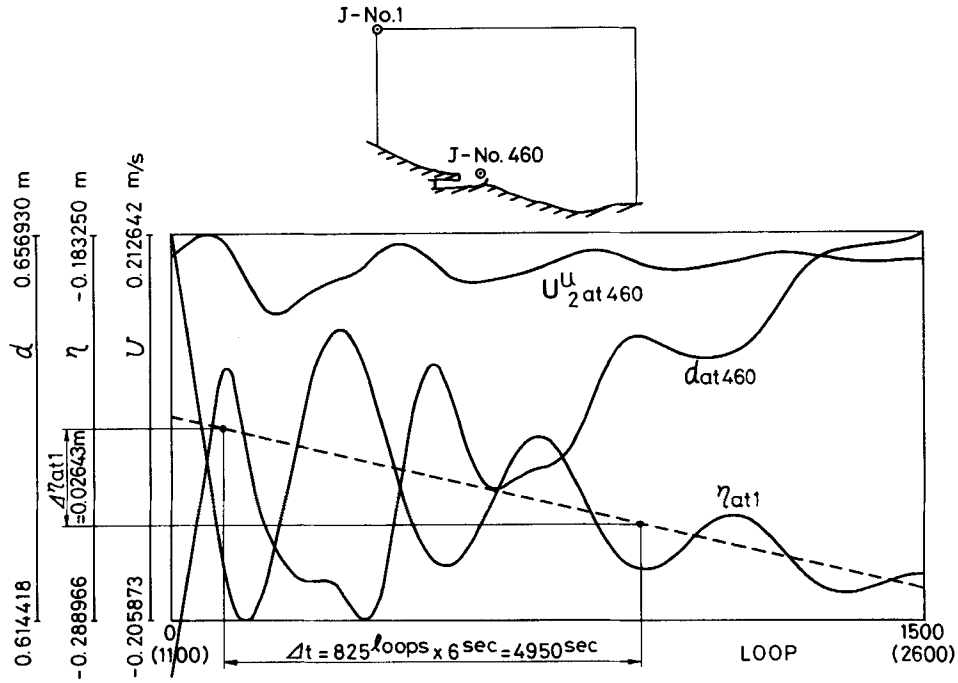


Figure 7. Time history curves of $U_2^u$, $\eta$ and $d$ (1st modification)

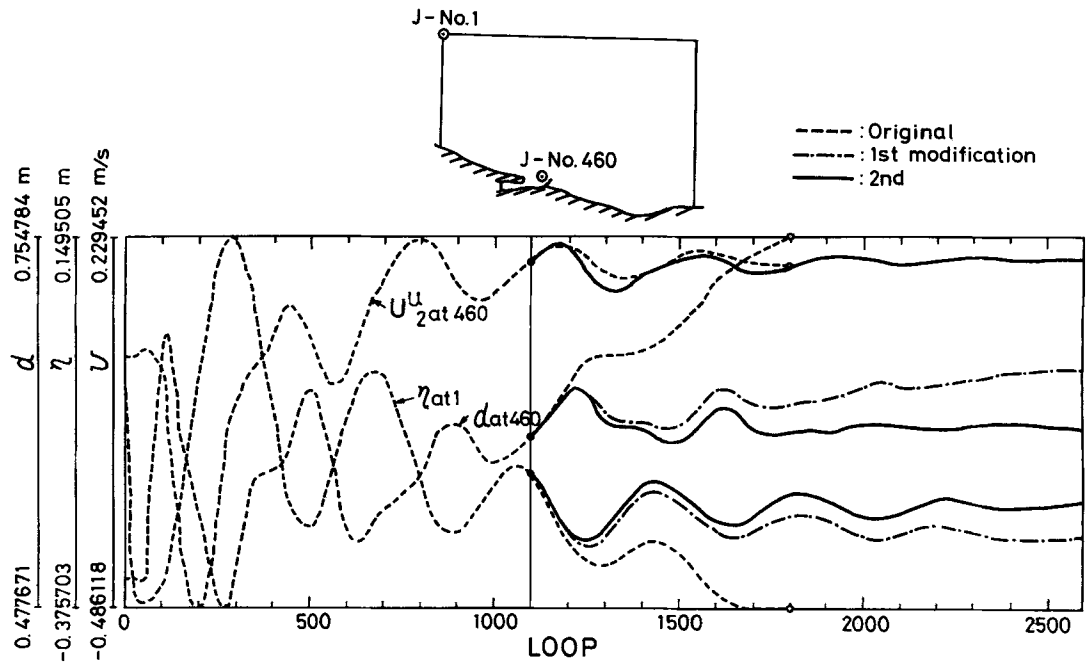


Figure 8. Time history curves of $U_2^u$, $\eta$ and $d$ (2nd modification)

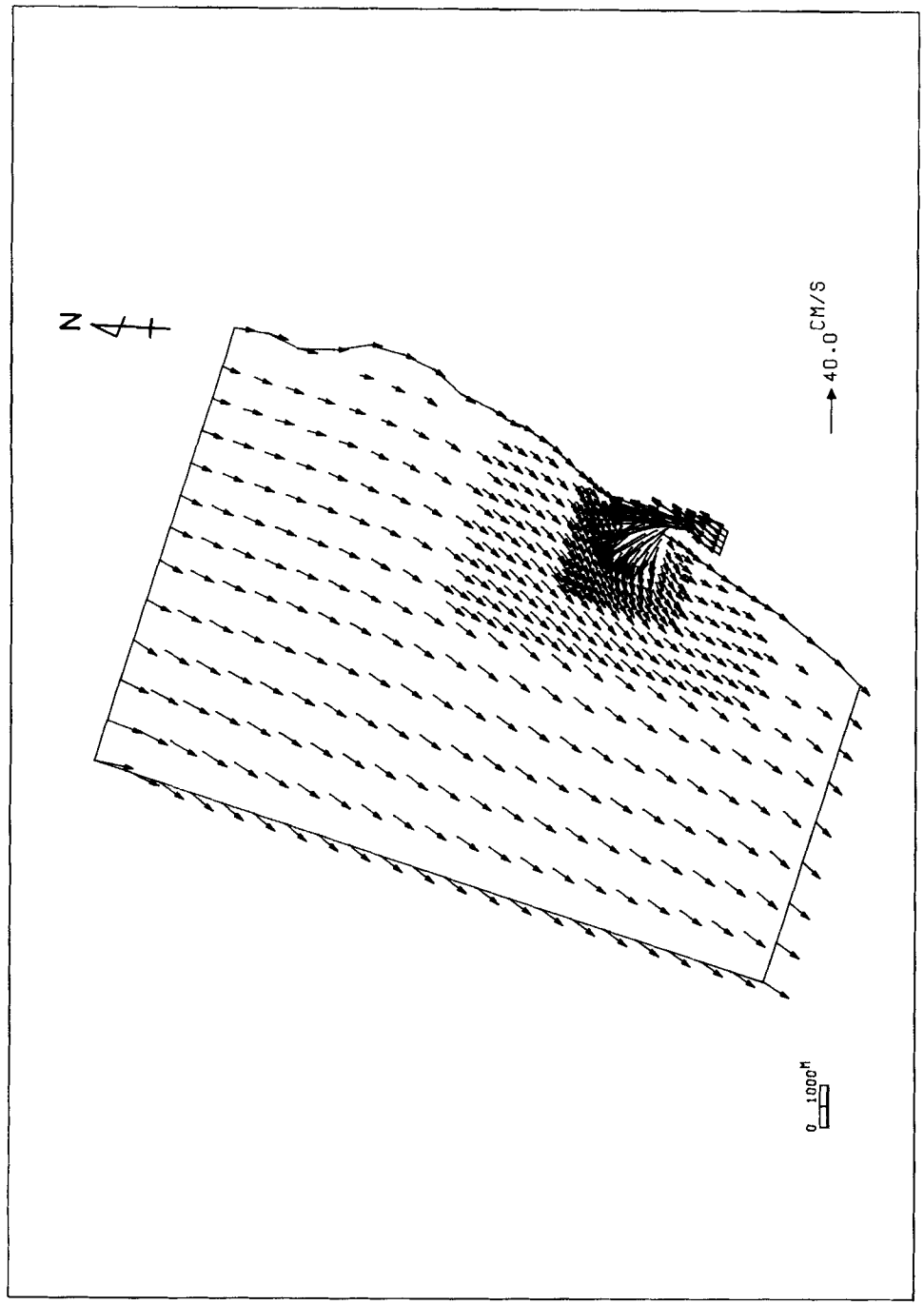


Figure 9. Computed velocities of upper layer

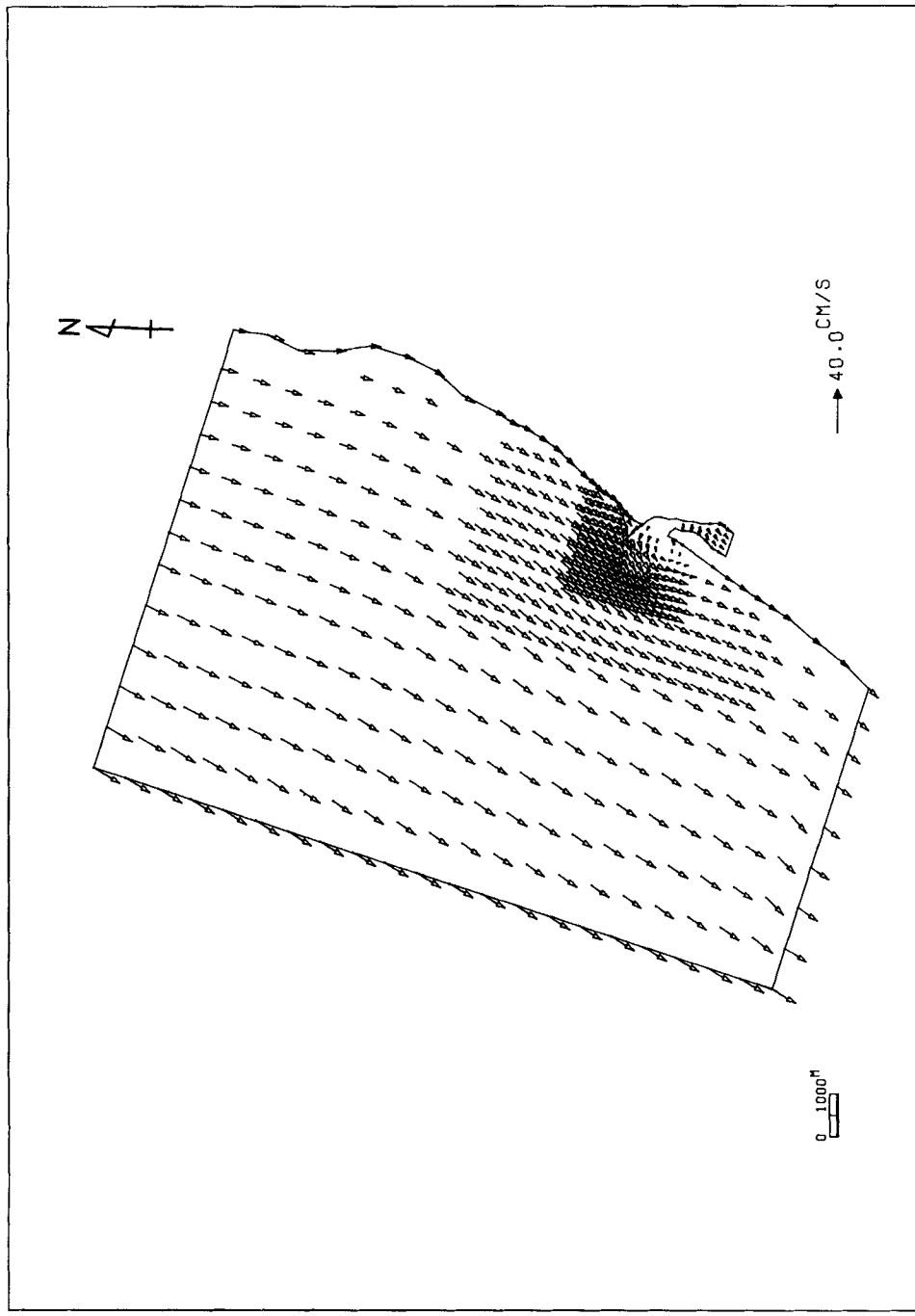


Figure 10. Computed velocities of lower layer

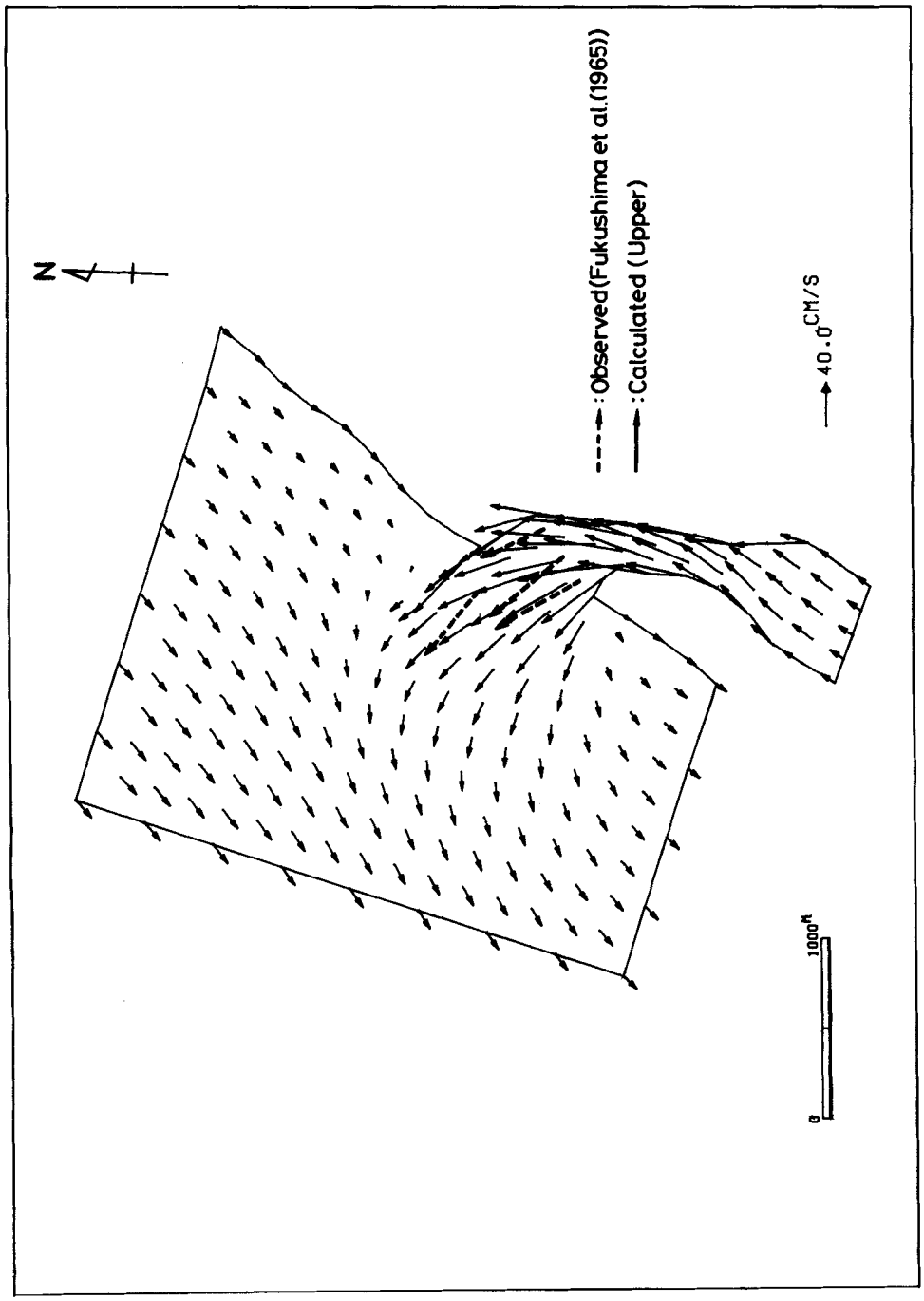


Figure 11. Computed velocities of upper layer (neighbourhood of estuary)

*Second modification*

Similarly, from the time history curve (Figure 7), $\Delta\eta$, $\Delta t$ snf $\dot{\eta}$ are obtained, i.e. $\Delta\eta_{at1} = 0{\cdot}02643$ m, $\Delta t = 825$ loops $\times$ 6 s $= 4950$ s. Therefore, the rate of surface water elevation change per unit time at nodal point No. 1 is $\dot{\eta}_{at1} = \Delta\eta_{at1}/\Delta t = 5{\cdot}34 \times 10^{-6}$ m/s. As an average for the whole region, the following value is assumed: $\dot{\eta} = 5 \times 10^{-6}$ m/s. Hence, $\dot{Q}_{st}/\dot{Q} = 1{\cdot}016$. Finally, the quantity adjustment should be 1·6 per cent above the first modification. As the initial condition, similar to the first modification, the result of loop No. 1100 of the original trial was used. Computation was carried out for more than 1500 loops under such conditions. Then, as shown in Figure 8, the water elevations $\eta$ and $d$ as well as the velocities can be used as a steady flow state.

## NUMERICAL RESULTS

Figures 9 and 10 represent the computed velocities of the upper and lower layers. Figure 11 shows the computed velocities of the upper layer (solid lines) in the neighbourhood of the estuary and the surface velocities observed by Fukushima *et al.*[26] (dotted lines). The velocity along the centre of flow is shown in Figure 12. They agree with each other very well. Figure 13 shows the computed velocities of the lower layer in the neighbourhood of the estuary. From these results, it can be seen that the flow of the upper layer and that of the lower layer are distinctly different, especially in the neighbourhood of the estuary. Figure 14 shows the distribution of the thickness of the upper layer, i.e. $\eta + d$. It shows that the upper layer decreases in thickness at the inlet and spreads over the bay in a very thin layer. Figure 15 is a comparison of the computed thicknesses of fresh water with the observed ones[27] in the neighbourhood of the estuary. The abscissa indicates the distance along the centre of flow from the inlet in the offshore direction, and the ordinate shows the thickness of fresh water, i.e. $\eta + d$, and river discharge is taken as a parameter. The computed result agrees with the observed data comparatively well.

## CONCLUSION

The finite element method has been applied to two-layer density flow analysis. As a time marching scheme, the explicit two-step selective lumping scheme was used. The present method is applied to the flow analysis of Ishikari Bay.

After several trials, it can be concluded that the numerical stability of the analysis depends significantly on combinations of the boundary conditions on the upper and lower layers. A method

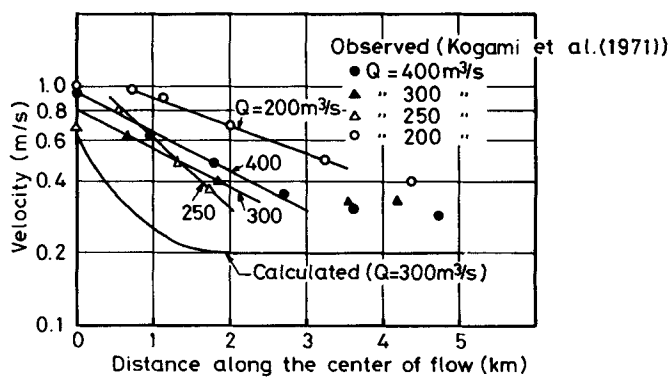


Figure 12. Comparison of computed velocity with observed surface velocities in the neighbourhood of the estuary

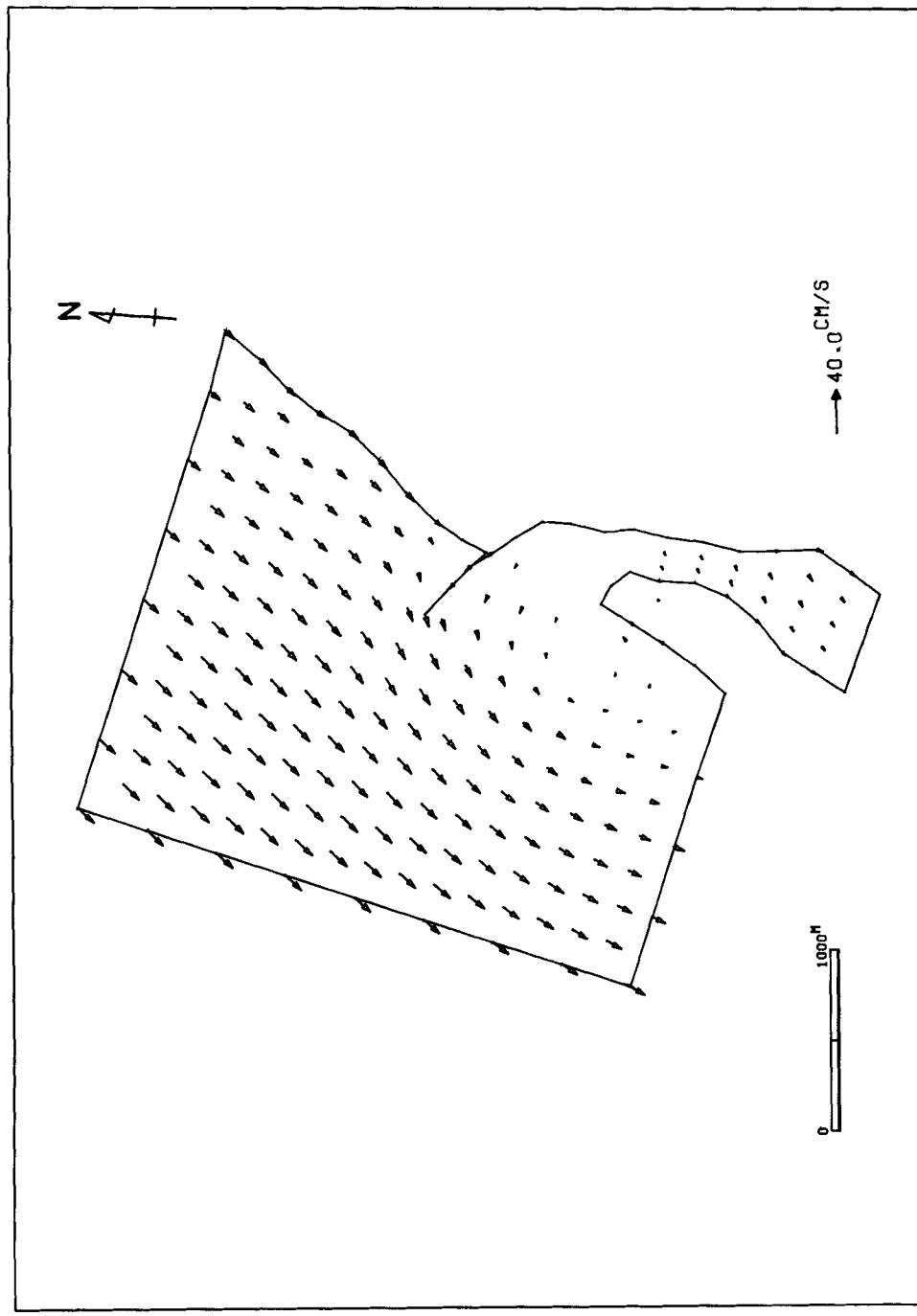


Figure 13. Computed velocities of the lower layer (neighbourhood of the estuary)

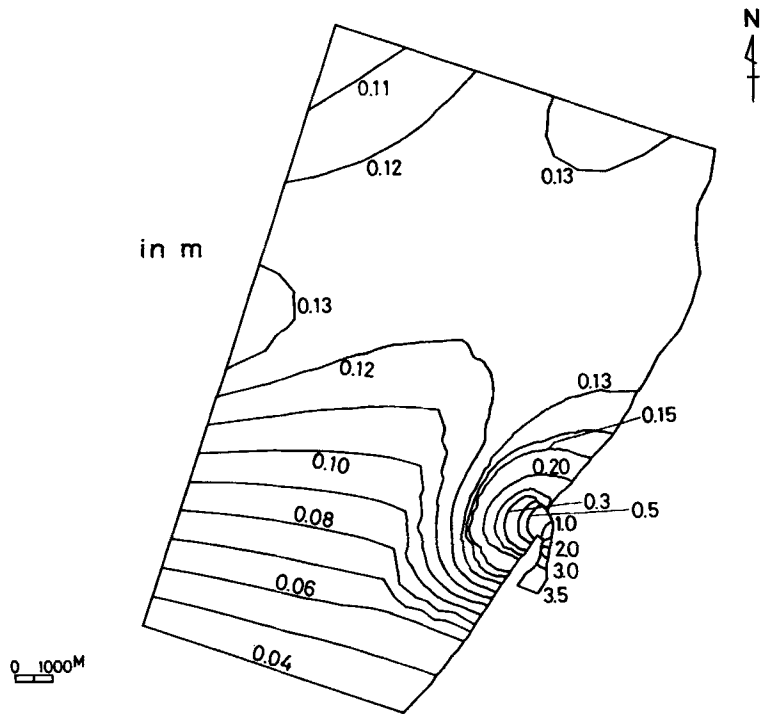


Figure 14. Distribution of thickness of upper layer ($\eta + d$)

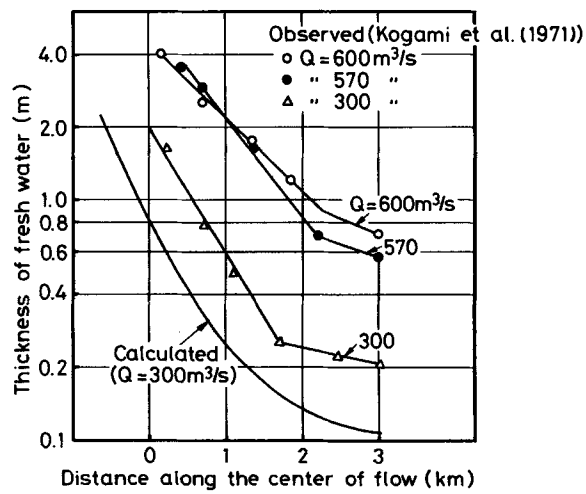


Figure 15. Comparison of computed thicknesses of fresh water with observed ones in the neighbourhood of the estuary

to obtain a stable solution is found by the combination, i.e. prescribing the thickness of the upper layer on the upper boundary and specifying the velocities on the lower boundary, and by the procedure of inflow adjustment. The computed results by the present method are in good agreement with the observed ones.

ACKNOWLEDGEMENTS

The authors gratefully acknowledge Mr. W. Fujiwara for coding some main modules of this program, and to Messrs. Y. Kodera, M. Itoh and Dr. M. Kishi of Mitsui Engineering & Shipbuilding Co., Ltd., for their kind advice and support during the preparation of this paper. The computation has been carried out using the IBM3033 Computer at Mitsui Engineering & Shipbuilding Co., Ltd.

REFERENCES

1. M. Kawahara and T. Okamoto, 'Finite element analysis of steady flow of viscous fluid using stream function', *Proc. JSCE*, No. 247, 123–135 (1976).
2. M. Kawahara, 'Steady and unsteady finite element analysis of incompressible viscous fluid', in *Finite Elements in Fluids* Vol. **3**, Wiley, Chichester, 1978.
3. M. Kawahara, 'Finite element methods of drift currents in coastal seas and estuaries using stream function', *TICOM Report, No. 78–11*, University of Texas at Austin, 1978.
4. O. C. Zienkiewicz, *The Finite Element Method*, 3rd edn, McGraw-Hill, London, 1977.
5. M. Kawahara, M. Morihira, S. Kataoka and K. Hasegawa, 'Periodic finite elements in two-layer tidal flow', *Int. J. Num. Meth. Fluids*, **1**, 45–61 (1981).
6. M. Kawahara and N. Kaneko, 'Periodic Galerkin finite element method of incompressible viscous fluid flow', in *Theoretical and Applied Mechanics*, Vol. **25**, University of Tokyo Press, 1977, 329–338.
7. M. Kawahara, 'Periodic Galerkin finite element method of unsteady flow of viscous fluid', *Int. J. Num. Meth. Engng.*, **11**, (7), 1093–1105 (1977).
8. M. Kawahara and K. Hasegawa, 'Periodic Galerkin finite element method of tidal flow', *Int. J. Num. Meth. Engng.*, **12**, 115–127 (1978).
9. M. Kawahara, Hasegawa and Y. Kawanago, 'Periodic tidal flow analysis by finite element perturbation method', *Comp. Fluid*, **5**, 175–189 (1977).
10. M. Kawahara and K. Hasegawa, 'Finite element analysis of two layered tidal flow', in L. C. Wellford, Jr. (Ed.) *Applications of Computer Methods in Engineering*, University of Southern California, 1977, pp. 1357–1366.
11. C. E. Peason and D. F. Winter, 'On the calculation of tidal currents in homogeneous estuaries', *J. Phys. Ocean.*, **7**, (6), 520–531 (1977).
12. S. Nakazawa, D. W. Kelly, O. C. Zienkiewicz, I. Christie and M. Kawahara, 'An analysis of explicit finite element applications for shallow water equations', in Norrie *et al.* (eds) *Proc. 3rd Int. Conf. Finite Element Methods in Flow Problems*, Vol. 2, 1980, pp. 1–12.
13. C. A. Brebbia and P. W. Patridge, 'Finite element simulation of water circulation in the North Sea', *Appl. Math. Model.*, **1**, (2), 101–107 (1976).
14. R. T. Cheng, 'Transient three-dimensional circulation of lakes', *Proc. ASCE*, **103**, (EM1), 17–34 (1977).
15. M. J. P. Cullen 'A simple finite element method for meteorological problems', *J. Inst. Math. Appl.*, **11**, 15–32 (1973).
16. W. G. Gray, 'An efficient finite element scheme for two dimensional surface water computation' in Pinder *et al.* (eds), *Finite Elements in Water Resources*, Princeton University, Pentech Press, 1976, pp. 433–449.
17. K. P. Holz and H. Hennlich, 'Numerical experiences from the computation of tidal waves by the finite element method', in Pinder *et al.* (eds), *Finite Elements in Water Resources*, Princeton University, Penetech Press, 1976, pp. 419–431.
18. J. R. Houston, 'Interaction of Tsunamis with the Hawaiian Islands calculated by a finite element model', *J. Phys. Ocean.*, **8**, 93–102 (1978).
19. P. W. Partridge and C. A. Brebbia, 'Quadratic finite elements in shallow water problems', *Proc. ASCE*, **102**, (HY9), 1299–1313 (1976).
20. J. Sündermann, 'Computation of barotropic tides by the finite element method', Pinder *et al.* (eds), *Finite Elements in Water Resources*, Princeton University, Penetech Press, 1976, 4–51–67.
21. D. L. Young and J. A. Liggett, 'Transient finite element shallow lake circulation', *Proc. ASCE*, **103** (HY2), 109–121 (1977).
22. J. D. Wang, 'Multi-level finite element hydrodynamic model of Block Island Sound', in Pinder *et al.*, (eds), *Finite Elements in Water Resources*, Princeton University, Penetech Press, 1976, pp. 469–493.
23. M. Kawahara, M. Kobayashi and K. Nakata, 'A three-dimensional multiple level finite element method considering variable water density', in R. H. Gallagher *et al.* (eds), *Finite Elements in Fluids*, Wiley, 1982, pp. 129–156.
24. M. Kawahara, H. Hirano, K. Tsubota and K. Inagaki, 'Selective lumping finite element method for shallow water flow', *Int. J. Num. Meth. Fluids*, **2**, 89–112 (1982).
25. H. Fukushima, I. Yakuwa, M. Takahashi and M. Ohtani, 'Mixing of salt water and fresh water at the estuary' (in Japanese), *Proc. 15th Coastal Engineering Conf.*, Japan Society of Civil Engineering, 185–190 (1968).
26. H. Fukushima, M. Kashimura, I. Yakuwa, M. Takahashi and M. Ohtani, 'A study in estuary of the Ishikari River (2nd Report)' (in Japanese), *Proc. 12th Coastal Engineering Conf.*, Japan Society of Civil Engineering, 158–161 (1965).
27. Y. Kogami, S. Nagauchi, F. Hoshi and M. Takamatsu, 'Sand drift in nearshore of Ishikari Bay' (in Japanese), *Proc. 18th Coastal Engineering Conf.*, Japan Society of Civil Engineering, 405–409 (1971).